Radiation calculations on the base of atmospheric models from lidar sounding

Irina Melnikova, Dmitry Samulenkov, Maxim Sapunov, Alexander Vasilyev, Anatoly Kuznetsov, and Victor Frolkis

Citation: AIP Conference Proceedings **1810**, 090006 (2017); doi: 10.1063/1.4975546
View online: http://dx.doi.org/10.1063/1.4975546
View Table of Contents: http://aip.scitation.org/toc/apc/1810/1
Published by the American Institute of Physics

Radiation Calculations on the Base of Atmospheric Models from Lidar Sounding

Irina Melnikova[1, 2 a)], Dmitry Samulenkov[1)], Maxim Sapunov[1)], Alexander Vasilyev[1)], Anatoly Kuznetsov[2)], Victor Frolkis[3, 4)]

[1]*St. Petersburg State University, Universitetskaya nab., 7/9, St. Petersburg, 199034, Russia*
[2]*Russian State Hydrometeorological University, Malookhtinsky pr., 98, St. Petersburg, 195196, Russia*
[3]*Emperor Alexander I St. Petersburg State Transport University, Moskovsky pr. 9, St Petersburg, 190031, Russia*
[4]*Voeikov Main Geophysical Observatory, Karbyshev ul., 7, St Petersburg, 194021, Russia*

[a)] i.melnikova@spbu.ru

Abstract. The results of lidar sounding in the Resource Center "Observatory of Environmental Safety" of the St. Petersburg University, Research Park, have been obtained in the center of St. Petersburg. Observations are accomplished during 12 hours on 5 March 2015, from 11 am till 11 pm. Four time periods are considered. Results of AERONET observations and retrieval at 4 stations around St. Petersburg region are considered in addition. Optical models of the atmosphere in day and night time are constructed from the lidar and AERONET observations and used for radiation calculation. The radiative divergence, transmitted and reflected irradiance and heating rate are calculated.

INTRODUCTION

Recently interest has arisen in the diurnal dynamics of radiative characteristics and especially in radiative forcing, and lidar sounding is applied toward the solution of the problem (Xu Hui et al., 2016). A study of the radiative regime under conditions of a big city is getting underway in St. Petersburg. The Resource Centre (RC) "Observatory of Environmental Safety" of the St. Petersburg State University (SPbSU) is located in the center of the city, on Vasilievsky Island, 10th Line, 33/35, at the height of 35 m, geographical coordinates Lat 59.943N, Lon 30.273E. It is equipped with aerosol and wind lidars, which provide information on the concentration, the physical nature and transfer of atmospheric aerosol in troposphere in the vertical direction. The results of the aerosol monitoring and retrieval during 12 hours on 5 March 2015 are analyzed. In addition, the data of 4 nearest AERONET stations situated around St. Petersburg are included into the consideration: Tøravere (Estonia), 5 and 6 March 2015, 262-km distance to St. Petersburg; Kuopio (Finland) 9 and 18 March, 2015, 357-km distance; Helsinki (Finland) 12 and 18 March, 2015, 300-km distance; and Moscow (Russia) 6 March, 2015, 637-km distance. The dates nearest to 5 March are taken, because the atmospheric conditions did not allow observation of the direct solar radiation at all the sites on the date considered. All the retrieved results, including aerosol optical thickness (AOT), single scattering albedo (SSA) and phase function asymmetry parameter, are used for optical modeling. Optical models for 4 time periods of lidar sounding are taken as a base for the calculation of solar radiation characteristics: reflection, transmission, radiative divergence, local radiative forcing, and heating rate.

Observational and inversion results

Here we demonstrate the results of the observation accomplished in the St. Petersburg center on 5 March 2015. Figure 1 shows an example of the vertical profile of the volume extinction coefficient $\alpha(z)$ in the height (m) – time (hour) coordinates, obtained from the 355-nm channel observation to the zenith direction, accomplished on 5 March 2015 during 12 hours. The figure clearly indicates a "pollution cap" above the city up to the height of 1.8 km. It is

Radiation Processes in the Atmosphere and Ocean (IRS2016)
AIP Conf. Proc. 1810, 090006-1–090006-4; doi: 10.1063/1.4975546
Published by AIP Publishing. 978-0-7354-1478-5/$30.00

seen that the extinction coefficient reaches maximal values from 15:30 till 17:30, and retains high values till 20:00. After 22:00 the extinction coefficient is 4 times less than in the day time and significantly dissipates and elevates.

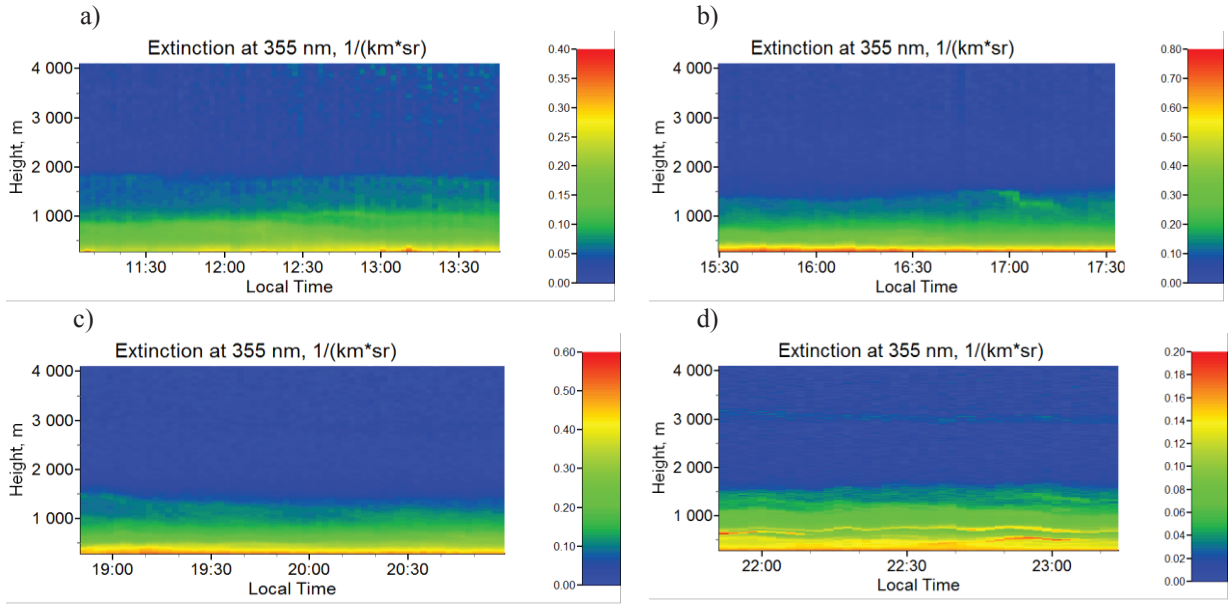

FIGURE 1. Dynamics of the aerosol extinction vertical profile variations during 12 hours from observations on 5 March 2015 in the 532-nm channel

The first task was to compare the aerosol optical thickness averaged over each time period with the AERONET results for validation of lidar sounding data. Regretfully, the St. Petersburg AERONET station situated in the suburb has not yet presented results to the network. Thus, we used the data of 4 surrounding AERONET stations ~300 km distant from St. Petersburg. The AOT values obtained on or about 5 March 2015 are presented in Table 1.

TABLE 1. Aerosol optical depth (km^{-1}) averaged over time intervals: 1 – 11:00-14:00, 2 – 15:30-17:30, 3 – 18:45-21:00 and 4 – 21:45-23:30 from lidar sounding and nearest AERONET stations

Data source, time	**Wavelength, nm**	340	355	440	500	532	1020	1064
Lidar, 11:00-14:00			0.129			0.167		0.022
Lidar, 15:30-17:30			0.302			0.182		0.033
Lidar, 18:45-21:00			0.247			0.147		0.021
Lidar, 21:45-23:30			0.113			0.119		0.014
AERONET, Tøravere (262km)								
5 March, 2015		0.339		0.296	0.246		0.199	
6 March, 2015		0.574		0.555	0.561		0.563	
AERONET, Kuopio (357km)								
9 March, 2015		0.051		0.043	0.039		0.028	
18 March, 2015		0.367		0.324	0.301		0.270	
AERONET, Helsinki (300km)								
12 March, 2015		0.028		0.024	0.021		0.014	
18 March, 2015		0.215		0.174	0.154		0.115	
AERONET, Moscow (637km)								
6 March, 2015		0.405		0.337	0.298		0.170	

The optical models for each of the 4 time periods are compiled from the observed and inversed data and presented in Table 2. The ground albedo is assumed equal to 0.7, because the snow covered the surface but in the city it was partly melted and removed. The optical thickness of the molecular scattering and absorption are taken from (Ginzburg et al., 2016). The SSA and asymmetry parameter g are from AERONET inversion results (http://aeronet.gsfc.nasa.gov/). The solar incidence angles θ corresponding to the time periods considered are 65, 70,

75, and 80°. The inhomogeneous model was constructed as modified Lowtran-6 with taking into account the vertical aerosol distribution from lidar sounding and air humidity from radiosounding on the same date.

TABLE 2. Optical model for radiative calculation

Time period	λ, nm	Aeros scat	Scat Sum	TAU aer	Rayl scat	Mol abs	TAU sum	SSA	*g*	A_s	F_0, W/m²/μ
Day-averaged	355	0.12	0.72	0.1285	0.60	0.001	0.730	0.9870	0.70	0.7	1000
Day-averaged	532	0.16	0.27	0.1635	0.11	0	0.277	0.9761	0.65	0.7	1790
Day-averaged	1064	0.02	0.07	0.0216	0.05	0	0.072	0.9777	0.60	0.7	650
1	355	0.10	0.70	0.1285	0.60	0.001	0.730	0.9596	0.70	0.7	1000
1	532	0.14	0.25	0.1666	0.11	0	0.277	0.9038	0.65	0.7	1790
2	355	0.20	0.80	0.3020	0.60	0.001	0.903	0.8859	0.70	0.7	1000
2	532	0.11	0.22	0.1824	0.11	0	0.292	0.8949	0.65	0.7	1790
3	355	0.20	0.80	0.2470	0.60	0.001	0.848	0.9434	0.70	0.7	1000
3	532	0.12	0.23	0.1470	0.11	0	0.257	0.9326	0.65	0.7	1790
4	355	0.10	0.70	0.1134	0.60	0.001	0.714	0.9798	0.70	0.7	1000
4	532	0.10	0.21	0.1187	0.11	0	0.229	0.9182	0.65	0.7	1790
	355				0.60	0.001	0.601	0.9983	0.70	0.7	1000
Without	532	0	0	0	0.11	0	0.11	1.0	0.65	0.7	1790
aerosols	1064				0.05	0	0.05	0.9777	0.60	0.7	650

Delta-Eddington approximation (Edd) and Monte-Carlo method (MC) with 1000000 photons analyzed are used for calculation of the radiative characteristics: the reflection $F^{\uparrow}$ at tropopause, transmission $F^{\downarrow}$ at the surface, and radiative divergence R in the troposphere for the 4 time periods as shown in Table 3. The radiative divergence is calculated by the formula: $dR=[(F^{\downarrow}-F^{\uparrow})_{top}-(F^{\downarrow}-F^{\uparrow})_{base}]/\Delta z$. The troposphere thickness is assumed Δz =10 km. The MC is applied for homogeneous and inhomogeneous atmosphere.

TABLE 3. Radiative characteristics

	λ, nm	$F\uparrow$	$F\downarrow$	*dR*	$F\uparrow$	$F\downarrow$	*dR*	$F\uparrow$	$F\downarrow$	*dR*	$F\uparrow$	$F\downarrow$	*dR*
θ			1: 65°			2: 70°			3: 75°			4: 80°	
Edd	355	0.673	0.778	0.009	0.528	0.583	0.030	0.653	0.610	0.016	0.758	0.609	0.006
homogen	532	0.649	0.868	0.009	0.641	0.815	0.011	0.683	0.802	0.008	0.680	0.726	0.010
MC	355	0.660	0.679	0.013	0.538	0.431	0.033	0.599	0.425	0.027	0.717	0.473	0.014
homogen	532	0.581	0.799	0.018	0.516	0.630	0.030	0.570	0.634	0.024	0.626	0.582	0.002
MC	355	0.676	0.684	0.012	0.618	0.441	0.025	0.671	0.453	0.019	0.775	0.466	0.009
inhomogen	532	0.585	0.800	0.012	0.538	0.630	0.027	0.591	0.627	0.022	0.643	0.596	0.018
						Without aerosols							
Edd	355	0.736	0.868	0.004	0.750	0.820	0.004	0.770	0.755	0.004	0.796	0.664	0.005
	532	0.710	0.966	0	0.715	0.951	0	0.628	0.925	0	0.736	0.879	0
MC	355	0.657	0.795	0.004	0.776	0.733	0.004	0.798	0.662	0.004	0.826	0.570	0.004
	532	0.707	0.959	0	0.714	0.934	0	0.727	0.895	0	0.748	0.825	0

The instantaneous direct aerosol forcing is defined as the difference between the net fluxes with (aer) and without (pur) aerosols at atmospheric top, base and atmosphere: $f_{top}=F^{\uparrow}_{aer}-F^{\uparrow}_{pur}$, $f_{base}=(1-A)(F^{\downarrow}_{aer}-F^{\downarrow}_{pur})$, $f_{atm}=f_{top}-f_{base}$ following (Xu Hui et al., 2016). The last expression indicates the difference in absorption of solar radiation in the atmosphere with and without aerosols. The values of the forcing during the day are presented in Table 4.

TABLE 4. Instantaneous spectral direct aerosol radiative forcing, W/m²/μ

	λ, nm	f_{top}	f_{base}	f_{atm}	f_{top}	f_{base}	f_{atm}	f_{top}	f_{base}	f_{atm}	f_{top}	f_{base}	f_{atm}
θ			1: 65°			2: 70°			3: 75°			4: 80°	
Edd	355	-25.4	-12.7	12.7	-99.2	-82.1	17.1	-31.1	-10.4	20.7	-7.0	-10.4	3.5
	532	-45.4	-22.7	22.7	-42.9	-85.7	42.9	27.8	-18.5	46.4	-18.7	-46.7	28.0
MC	355	1.27	-14.8	16.1	-81.9	-31.4	50.6	-51.7	-18.45	33.3	-18.9	-5.0	13.9
homogen	532	-81.0	-121.2	25.9	-68.2	-186.7	65.1	-73.0	-121.36	48.3	-37.9	-75.5	37.6
MC	355	-8.07	-14.7	6.63	-54.4	-30.3	24.1	-33.0	-54.3	21.3	-8.86	-18.1	9.2
inhomogen	532	-92.2	-120.8	28.1	-108.5	-186.9	78.4	-63.4	-124.9	61.5	-32.7	-71.3	38.5

It is seen that in UV ranges negative forcing is retained all the day except for the atmospheric forcing f_{atm} in the evening. The radiative forcings f_{top} and f_{atm} in visual channel change the minus to plus sign, but f_{base} is negative during

the day. The day-averaged and approximately spectrally integrated values of the direct radiative forcings are shown in Table 5. The inhomogeneous model provides higher values of the direct forcing in most cases.

TABLE 5. Direct total aerosol forcing, W/m^2

λ, nm	355	532	1064	Total
f_{top}	-1.62	-0.48	-0.14	-1.3
f_{base}	-3.81	-12.4	-0.88	-5.0
f_{atm}	2.23	11.9	0.74	7.5

Similar estimates of the instantaneous direct aerosol forcing were obtained with making use of Eddington approximation including the radiation code (Frolkis and Rozanov, 1993) based on the 26-layer radiative-convective atmospheric model.

The day aerosol forcing of the atmosphere (radiation absorption) calculated on the base of the model from the day-averaged data is positive at the three considered wavelengths and total. The forcings at the top and base of the atmosphere are negative.

The solar shortwave heating rate is defined in the conventional manner: $\left(\frac{dT}{dt}\right)_p = \frac{S_\lambda}{rC_p} dR$

S_λ = 1380 W/m^2 – Incident solar flux in shortwave ranges (0.3–1.0 μ);
r = 1 kg/m^3 – Air density at the level of 800 mbar;
C_p = 1005 J/(kg deg) – Specific heat of dry air at a constant pressure

For the light day duration of 7 hours the heating rate appears to be about 0.3 deg/h.

CONCLUSION

The optical atmospheric model based on the results of lidar sounding of the atmosphere together with the Eddington approximation provides an adequate estimate of the diurnal variations of the spectral and total radiation characteristics including direct radiative forcings that appeared close to the values obtained earlier (Xu et al., 2016; Mallet et al., 2015; Frolkis and Rozanov, 1993).

ACKNOWLEDGMENTS

The equipment of the Resources Centre “Observatory of Environmental Safety” of Research Park, St. Petersburg State University, was used in the study.

REFERENCES

1. Donchenko V., Boreisho A., Chugreev A., Melnikova I., Samulenkov D. Current problems in remote sensing of the Earth from Space. Moscow **10**, 122–132, 2013 (In Russian).
2. Veselovskii I., Whiteman D.N., Kolgotin A., Andrews E., Korenskii M. J. of Atmos. and Ocean. Tech. **26**, 1543–1557, 2009.
3. H. Xui, J. Guo, X. Ceamanos, J.-L. Roujean, M. Min, D. Carrer, Atmosph. Envir., 141, 186–196, 2016.
4. G. I. Gorchakov, M. A. Sviridenkov, Atmospheric and Ocean Physics, **15**, 53–59, 1979 (Bilingual).
5. F. X. Kneizis, L. W. Abreu, G. P. Anderson, G. H. Chetwynd, E. P. Shettle, A. Berk, L. S. Bernstein, D. S. Robertson, P. Acharya, L. S. Rothman, J. E. A. Selby, W. O. Gallery, S. A. Clouth, *The Modtran 2/3. Report and Lowtran 7 model.* (Phillips Laboratory, Hanscon, Massachusetts, 1996), 230 p.
6. V. Frolkis, E. Rozanov, “Radiation code for climate and general circulation models”, in *Current problems in Atmospheric Radiation,* IRS'92 Proceedings edited by S. Keevallik (A.DEEPAK Publ. Hampton, USA, 1993), pp.176–179.
7. A. Ginzburg I., Melnikova, S. Novikov, V. Frolkis, Current problems in remote sensing of the Earth from Space. Moscow, 2016 (In press, Bilingual).